Systematic Mutational Analysis of the Yeast *ACT1* Gene

Kenneth F. Wertman,*[,1] David G. Drubin[†] and David Botstein*[,2]

**Genentech, Inc., South San Francisco, CA 94080, and [†]Department of Molecular and Cell Biology, University of California, Berkeley, California 94720*

Manuscript received March 9, 1992
Accepted for publication June 10, 1992

ABSTRACT

We report the isolation and characterization of a synoptic set of site-directed mutations distributed throughout the single actin gene of *Saccharomyces cerevisiae*. Mutations were systematically targeted to the surface of the protein by identifying clusters of 2 or more charged residues in the primary sequence; every charged residue in a cluster was replaced with alanine. Mutations were recovered in high yield (34 of 36 constructed) as heterozygous diploids. Mutant phenotypes were examined in haploid segregants: 11 were recessive lethal, 16 conditional-lethal (including temperature-sensitive and salt-sensitive) and 7 had no discernible phenotype. Genetic analysis suggested that the two mutations constructed but not recovered in yeast may have a dominant defective phenotype. Location of the mutant residues on the three-dimensional structure of the rabbit muscle actin monomer confirmed that most (81%) of the charged residues we altered lie at or near the surface of the protein, confirming a key assumption of the method. Many of the new *act1* alleles have properties readily interpreted in light of the actin structure and should prove useful in both genetic and biochemical studies of actin function.

IN eukaryotic cells, the actin cytoskeleton underlies numerous fundamental processes, including cell motility, cytoplasmic streaming, cytokinesis and organization of the cell surface and extracellular matrix. Actin does not function alone. Numerous proteins have been isolated from diverse sources that influence actin assembly or change the physical properties of actin filaments (POLLARD and COOPER 1986). Presumably, it is through the integration of these many activities that cells achieve proper spatial and temporal control over actin assembly and function.

Yeast has proven to be a tractable organism for studying the actin cytoskeleton, especially the identification and characterization of proteins that interact functionally with actin. There is just one structural gene for actin (*ACT1*). The deduced primary sequence of yeast actin is 88% identical to mammalian muscle or cytoplasmic actins (NG and ABELSON 1980; GALLWITZ and SUERS 1980). Yeast cells serve as a convenient source for the purification of a single actin isotype (GREER and SCHECKMAN 1982), and it has recently been shown (KRON 1990; KRON *et al.* 1992) that yeast actin filaments will move on glass slides coated with rabbit muscle myosin. *ACT1* was shown genetically to be an essential gene (SHORTLE, HABER and BOTSTEIN 1982) and two conditional-lethal alleles (*act1-1* and *act1-2*, both temperature-sensitive) were obtained by *in vitro* mutagenesis and gene replacement techniques (SHORTLE, NOVICK and BOTSTEIN 1984). The phenotypes of these two alleles are not identical; they were studied extensively (NOVICK and BOTSTEIN 1985), with results that implicated actin as being necessary for proper cell morphology (especially polarity of cell surface growth) as well as organization and secretion of materials to and through the plasma membrane.

Suppression of the two *act1* alleles yielded a number of new genes (*SAC1-SAC6*) whose products might interact functionally with actin (NOVICK, OSMOND and BOTSTEIN 1989; ADAMS and BOTSTEIN 1989). Two of these (*SAC1* and *SAC6*) have been studied further. *SAC1* encodes a protein that is implicated in secretory processes (CLEVES, NOVICK and BANKAITIS 1989). *SAC6* encodes the yeast homologue of fimbrin, a well characterized actin-bundling protein in mammalian cells (ADAMS, BOTSTEIN and DRUBIN 1991).

This success in finding functionally interacting genes by genetic methods starting with just two *act1* alleles and the strong expectation, based on other eukaryotic cells, that there are many more actin-binding proteins to be found in yeast has stimulated attempts to isolate more conditional-lethal alleles of *ACT1*. The method used originally by SHORTLE, NOVICK and BOTSTEIN (1984), although quite useful with other proteins (HOLM *et al.* 1985; HUFFAKER, THOMAS and BOTSTEIN 1988) has consistently yielded surprisingly few conditional-lethal actin alleles; extensive further application of this technique yielded only one

[1] Present address: Department of Molecular and Cell Biology, University of California, Berkeley, California 94720. To whom correspondence should be addressed.
[2] Present address: Department of Genetics, School of Medicine, Stanford University, Stanford, California 94305.

additional mutation (act1-4; T. DUNN and D. SHORTLE, unpublished result). Two of the three existing mutations lie at sites now known to be within a single subdomain of the folded protein (*act1-1* changes a proline at residue 32 to leucine [or by convention, P32L] and *act1-2* changes alanine at residue 58 to threonine [A58T]); the third is far removed from the first two (glutamate 259 to valine [E259V]). These three should represent only a small fraction of the many potential binding and other functional domains of the protein.

Recently, powerful general techniques for systematic mutagenesis of protein coding sequences have been developed. These were aimed in the first instance at *in vitro* biochemical studies of the proteins, for which it was desired to alter the surface of functional domains one at a time, with minimal misfolding or structural alterations at a distance from the altered site. The first of these was called "alanine-scanning mutagenesis" and was used by CUNNINGHAM and WELLS (1989) to map the residues that are responsible for the binding between human growth hormone and its receptor. These authors argued that alanine substitutions are relatively conservative at virtually any residue that is not buried deep in the hydrophobic core of the structure. Their argument was buttressed by their experience: most of the mutations they made were expressed as stable proteins that could readily be purified and studied.

A variant of this method, called "clustered charged-to-alanine scanning mutagenesis" has since been developed that is particularly effective in systematically studying all the domains on the surface of proteins, even ones that are very large (BENNETT *et al.* 1991; BASS, MULKERRIN and WELLS 1991; GIBBS and ZOLLER 1991). In this procedure, one attempts to survey with mutations the surface of the protein by exploiting the fact that clusters of charged residues are generally not accommodated in buried structure. One finds the clusters in the sequence with an algorithm–for instance all cases in which 2 or more charged residues are found in a stretch (or "window") of 5 residues. Each cluster is then changed by site-directed methods so that all of the 2–5 charged residues are changed to alanine. Thus, the significant portion of the protein's surface can be surveyed in a relatively unbiased and nondestructive way with a relatively small number of constructed mutants. The success of this approach is illustrated by the experience of BENNETT *et al.* (1991), who found that 90% of the clustered charged-to-alanine mutants spanning the entire 527 residues of human tissue plasminogen activator (tPA) expressed stable, properly folded mutant proteins that could be studied by the same methods used for wild-type protein.

In this paper we present a clustered charged-to-alanine scan of yeast actin. However, instead of assessing the residual function of mutant proteins by biochemical means, we have assessed the phenotype caused by the mutations *in vivo*, by gene replacement of the *ACT1* gene with the mutations. A marked diploid strain was transformed with each of the mutations and the phenotype of the mutants assessed after tetrad dissections. Care was taken to verify directly, wherever possible, the presence of the mutations in the transformants. We recovered 34/36 mutations, among which we found a number of recessive-lethals (11), and a surprising number of recessive conditional lethals (16) and mutations with no discernible phenotype (7).

MATERIALS AND METHODS

Plasmid construction: All DNA manipulations were performed by standard techniques (MANIATIS, FRITSCH and SAMBROOK 1982). Restriction endonucleases and other enzymes were obtained from New England Biolabs (Beverly, Massachusetts) with the exception of *Taq* Polymerase (Cetus-Perkin Elmer). A 3.8-kb *ACT1*-containing genomic *Eco*RI fragment (see Figure 2A) from pRB155 (SHORTLE, NOVICK and BOTSTEIN 1984) was inserted into the *Eco*RI site of the *Escherichia coli* vector pUC119 (VIEIRA and MESSING 1991). One construct (pKFW41) contained *ACT1* oriented with respect to M13 *ori* such that superinfection with M13 helper phage results in the production of encapsidated single stranded plasmid containing the antisense strand of *ACT1*. This plasmid was propagated on an adenine methylase deficient strain (GM33; provided by M. MARINUS, University of Massachusetts Medical School) and used to construct the following plasmids.

A selectable marker was inserted in the genomic sequences downstream of *ACT1* by digestion of pKFW41 with *Bcl*I and ligation to a *HIS3* containing *Bam*HI fragment obtained from YCp404 (MA *et al.* 1987). A recombinant with *HIS3* transcription oriented away from the *ACT1* gene (pKFW46) was used for all subsequent experiments. The structure of the resulting *Eco*RI insert is depicted in Figure 2C in its genomic context. Uracil containing single stranded pKFW46 DNA was produced by infection of KW311 (CJ236:*dut*$^-$ *ung*$^-$/pKFW46) with M13KO7 (VIEIRA and MESSING 1987).

A plasmid-borne *LEU2* marked *act1* deletion allele (*act1Δ1::LEU2*) was constructed by digestion of pKFW41 DNA with *Bcl*I and *Xho*I and ligation in the presence of a *LEU2* containing *Bam*HI/*Sal*I fragment derived from YCp409 (MA *et al.* 1987). This construct (pKFW48) removes all *ACT1* coding information except for the first three amino acid residues. The resulting structure of the *Eco*RI fragment is depicted in Figure 2B in its genomic context.

Oligonucleotide-directed mutagenesis: Thirty-six synthetic oligonucleotides were used to change 75 selected charged amino acids in yeast actin to alanine. Oligonucleotides were designed to contain at least 12 and 9 nucleotides of perfect homology on the 5′ and 3′ sides, respectively, of the mutant sites. In some cases the 3′ homology was lengthened to reduce the likelihood of priming at secondary sites in the known plasmid sequence or to increase the guanine and cytosine content of the duplex regions to approximately 50%. After phosphorylation with T4 polynucleotide kinase, oligonucleotides (8 ng) were used to prime DNA synthesis by T4 DNA polymerase (1 unit) on single stranded uracil

TABLE 1

Yeast strains

Strain	Genotype
KWY158	*MAT***a** *ura3-52 leu2-3,112 his3Δ200 act1-2*
KWY161	*MATα ura3-52 leu2-3,112 his3Δ200 act1-3*
KWY167	*MAT***a** *ura3-52 his3Δ200 act1-4*
KWY175	*MATα ura3-52 leu2-3,112 his3Δ200 tub2-201 ade4 act1-3*
DBY3357	*MAT***a** *ura3-52 leu2-3,112 his3Δ200 ade2-101(am) can1 cry1*
KWY198	KWY175 × DBY3357
KWY201	KWY198 transformed with pKFW48 (see text)

The mutants described here were all isolated from KWY201; a list of alleles and strain numbers appears in Figure 7.

containing pKFW46 DNA (0.6 μg) in the presence of T4 DNA ligase (200 units) using the buffers and temperature regimens described by KUNKEL, ROBERTS and ZAKOUR (1987). Mutant plasmids were recovered by calcium chloride mediated transformation of the *ung*$^+$ *E. coli* strain BSJ72 (*supE, hsdΔ5, thi (Δlac-proAB)* λ^r *Sm*^{r} *F′ [traD36 proAB*$^+$ *lacI*^{q} *lacZΔM15]*). Transformation reactions were divided into two independent pools prior to plating at 37° on LB agar containing carbenicillin (50 μg/ml). Mutant plasmids were identified using restriction site polymorphisms introduced by the alanine codon substitutions (often involving the enzyme Fnu4HI, see Figure 4). Dideoxy-chain termination DNA sequencing (SANGER, NICKLEN and COULSON 1977) was used to confirm replacements that did not alter plasmid restriction sites. At least two independent bacterial transformants bearing mutant plasmids were recovered for each allele; overall, 67% of the bacterial plasmids analyzed contained the desired substitution. In most cases (see Table 2 below) two or more such independent plasmids were used to construct yeast strains; all such duplicates turned out to have identical properties

Yeast strain construction: The strains used in these studies are derivatives of S288C and are listed in Table 1 and below (see *Allele Replacement at ACT1*). The cultivation and manipulation of yeast strains followed standard methods (ROSE, WINSTON and HIETER 1990). Yeast cell transformation was performed by the Li-acetate method (ITO *et al.* 1983). Yeast strains were sporulated in SPM medium at 26° with vigorous aeration as described by KASSIR and SIMCHEN (1991). Auxotrophic markers were scored after 3 days of incubation at 25° on SD agar plates containing all but one of the nutrients required to supplement the auxotrophies (histidine, leucine, uracil, adenine). The *ade2* and *ade4* mutations were distinguished by mating haploids to lawns of marked tester strains (admixtures of *MAT***a** and *MATα* cells bearing either *ade2* or *ade4* mutations) on SD agar containing histidine, leucine and uracil. All temperature growth range experiments were performed by spotting cell suspensions on YEPD agar (unless otherwise stated). These plates were incubated at the various temperatures and scored at a time deemed appropriate by comparison to wild-type control strains.

The transformation strain (KWY201), was constructed in a two step process. First, DBY3357 was mated to KWY175 yielding a strain KWY198 as depicted in Figure 2A. This strain was heterozygous (*act1-3 tub2-201/ACT1 TUB2*) at the closely linked *ACT1* and *TUB2* locus; the *tub2-201* allele confers recessive resistance to the antimicrotubule drug benomyl (Ben) but no other phenotype. Transformation of this diploid with *Bam*HI digested (and phenol chloroform extracted) pKFW48 plasmid DNA yielded Leu$^+$ transformants at 26° on SD medium supplemented with histidine and uracil. Tetrads derived from these transformants were dissected (SHERMAN and HICKS 1991) on YEPD medium and incubated at 26°. Cell suspensions of haploid segregants from these dissections were spotted on YEPD agar at various temperatures, and appropriately supplemented SD agar, to identify those in which the temperature sensitive *act1-3* allele had been replaced with the *LEU2* insertion/deletion at the *act1* locus (Figure 2B). This was indicated by 2:2 segregation of lethality, and all surviving spores being Ts$^+$, Leu$^-$, and benomyl sensitive. Of six transformants analyzed, five met these criteria. One of these (KWY201) served as the transformation recipient for all allele replacement experiments (see RESULTS).

Allele replacement at *ACT1*: Derivatives of pKFW46 bearing oligonucleotide generated mutations were used to replace the *act1Δ1::LEU2* allele in KWY201 by Li-acetate-mediated DNA transformation. Transforming DNA was prepared by restriction endonuclease digestion of the transforming plasmid DNA with *Eco*RI and the release of the *HIS3* marked *act1* containing fragment was confirmed by agarose gel electrophoresis. These digests were heat treated at 70° for 20 min and stored frozen prior to use in yeast tranformations. Transformants were recovered by incubation on SD medium supplemented with leucine and uracil at 26°. His$^+$ transformants were replica plated to SD supplemented with uracil, either with or without leucine, to identify those that had lost the *LEU2* marker.

The following diploid strains were recovered by screening transformants of KWY201 in the manner described above. Each contains the indicated *act1* allele replacing *act1Δ1::LEU2*: (KWY241,*act1-101::HIS3*); (KWY242,*act1-102::HIS3*); (KWY246,*act1-103::HIS3*); (KWY248,*act1-104::HIS3*); (KWY249,*act1-105::HIS3*); (KWY251,*act1-106::HIS3*); (KWY253,*act1-107::HIS3*); (KWY254,*act1-108::HIS3*); (KWY255,*act1-109::HIS3*); (KWY257,*act1-110::HIS3*); (KWY258,*act1-111::HIS3*); (KWY260,*act1-112::HIS3*); (KWY261,*act1-113::HIS3*); (KWY262,*act1-115::HIS3*); (KWY263,*act1-116::HIS3*); (KWY264,*act1-117::HIS3*); (KWY265,*act1-118::HIS3*); (KWY266,*act1-119::HIS3*); (KWY268,*act1-120::HIS3*); (KWY269,*act1-121::HIS3*); (KWY271,*act1-122::HIS3*); (KWY273,*act1-123::HIS3*); (KWY277,*act1-124::HIS3*); (KWY278,*act1-125::HIS3*); (KWY279,*act1-127::HIS3*); (KWY281,*act1-128::HIS3*); (KWY283,*act1-129::HIS3*); (KWY285,*act1-130::HIS3*); (KWY286,*act1-131::HIS3*); (KWY288,*act1-132::HIS3*); (KWY289,*act1-133::HIS3*); (KWY290,*act1-134::HIS3*); (KWY291,*act1-135::HIS3*); (KWY293,*act1-136::HIS3*); (KWY295,*ACT1::HIS3*).

Polymerase chain reactions (PCR), employing standard conditions (SAIKI *et al.* 1988), were used to confirm coinheritance of *HIS3* and the mutant alleles by priming synthesis with an *ACT1* upstream sense strand primer

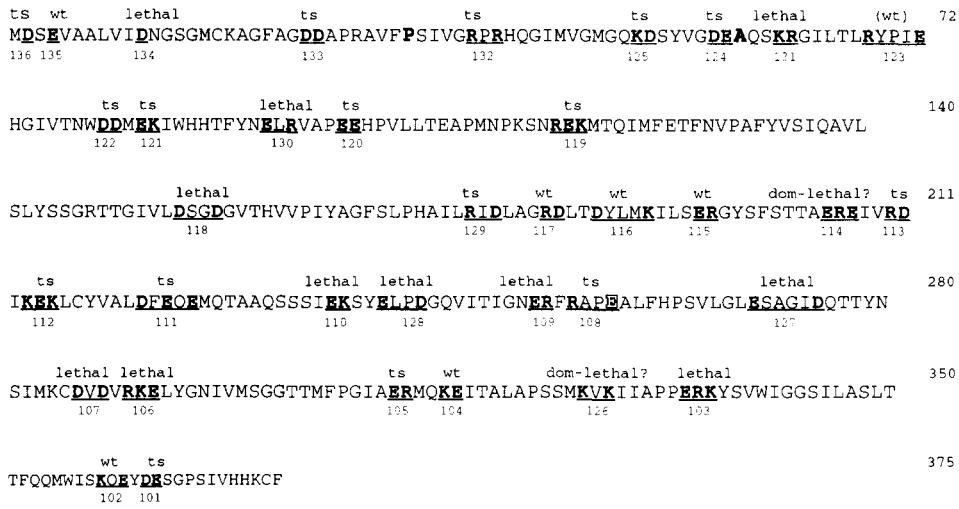

FIGURE 1.—Positions of charged-clusters replaced with alanine. The deduced single-letter code amino acid sequence of the yeast actin protein indicating the positions of all known mutations. The "charged-clusters" that were modified in these experiments are underlined (with allele numbers below), and the residues that were replaced with alanine are presented in boldface type. The phenotype of haploid cells containing each mutation is indicated above the sequence. The three previously identified temperature sensitive mutations are shown with hollow letters: *act1-3*, P32L and *act1-2*, A58T (SHORTLE, NOVICK and BOTSTEIN 1984); *act1-4*, E259V (T. DUNN and D. SHORTLE, personal communication).

(5′CCGGATCCTTCCACGTCCTCTTGC-3′) and a *HIS3* upstream antisense primer (5′CCGGATCCGGAAACGTTGAATGAAGAC-3′). Genomic DNA (1 μl/50 μl reaction) used for these experiments was prepared by the procedure of HOFFMAN and WINSTON (1987) except the detergent concentration in the buffer, STES, was reduced to 0.1%.

RESULTS

The overall plan of our experiments was to identify clusters of charge in the deduced amino acid sequence of the *ACT1* gene, to change all the charged residues to alanine to make a single mutation for each cluster, to replace one of the actin genes in a diploid with each of the mutations, to dissect the heterozygotes and to assess the phenotype of the spores carrying each of the clustered charged-to-alanine mutations. To do this rigorously and efficiently we built means of recognition and verification into the mutations, the plasmid vectors and the recipient yeast diploids so that we could select for and/or monitor the presence of the mutations at each step.

Design and construction of the mutations: The algorithm we used (with a few exceptions) was two or more charges in a window of five. The amino acid changes effected by the 36 mutations we made are illustrated in Figure 1. The only exceptions to the algorithm were that we split the amino-terminal cluster, constructing D2A and E4A (*i.e.*, $asp_2 \rightarrow$ ala and $glu_4 \rightarrow$ ala) as separate mutations, and we constructed E270A,D275A even though these residues span a window of six.

Oligonucleotide-directed mutagenesis was done by the method of KUNKEL, ROBERTS and ZAKOUR (1987) as described in MATERIALS AND METHODS. When ever possible, the oligonucleotide sequence was designed to make the mutation verifiable by restriction digest. Often the mutations required changing adjacent charged residues to alanine (codons GCN GCN) automatically created an Fnu4H1 recognition site (GCNGC). In other cases, we chose sequences so that other restriction sites were created or destroyed by the mutations (see Table 2; "Detection"). Occasionally no site could be created or destroyed, and then verification was possible only by DNA sequence (6/36), occasionally causing some uncertainty in yeast (see below). All of the mutations we made were verified by restriction digest and/or DNA sequencing at the plasmid stage.

Insertion of the mutations into yeast diploids: The plasmid vector (pKFW46, See MATERIALS AND METHODS and Figure 2) in which the mutagenesis was done contains the entire *ACT1*-coding sequence and also contains a functional *HIS3* gene inserted into a *Bcl*I site downstream of the *ACT1* transcriptional terminator (GALLWITZ, PERRIN and SEIDEL 1981). The *HIS3* and *ACT1* genes are transcribed in the same direction. The *HIS3* gene was provided to allow for selection by linkage, after transformation of yeast, of the adjacent *ACT1* coding sequence whose end is only ≈300 nucleotides distant. The addition of the *HIS3* DNA also provides a DNA size change at the *ACT1* locus that allows verification (by Southern blot) of the integration of the construction at that locus. Haploid and diploid strains carrying this construction with an otherwise unmutagenized *ACT1* gene grow normally (Figure 3 and see below).

If one were simply to use an ordinary diploid with two copies of the *ACT1* gene as recipient for transformations with the mutations, selecting the adjacent

TABLE 2

Experimental summary

Amino acid replacement	Allele[a]	Haploid phenotype[b]	Dominance	Detection[c]	No. analyzed[d]	Tetrads dissected[e]
None	*ACT1*	Wild type			3	12, 12, 12
DA2	*act1-136*	Cs$^-$, Ts$^-$[f]	Recessive	*Hin*FI (−)	3	10, 8, 8
E4A	*act1-135*	"Wild type"		*Mnl*I (−)	2	20, 8
D11A	*act1-134*	Lethal	Partial dominant	DNA sequence	1	10
D24A,D25A	*act1-133*	Cs$^-$, Ts$^-$	Recessive	Fnu4HI (+)	1	10
R37A,R39A	*act1-132*	Cs$^-$, Ts$^-$	Recessive	*Acc*I (−)	1	10
K50A,D51A	*act1-125*	Cs$^-$, Ts$^-$	Recessive	Fnu4HI (+)	1	8
D56A,E57A	*act1-124*	Ts$^-$	Recessive	*Pst*I (+)	1	8
K61A,R62A	*act1-131*	Lethal	Partial dominant	Fnu4HI (+)	1	8
R68A,E72A	*act1-123*	"Wild type"		DNA sequence	4	10, 8, 10, 9
D80A,D81A	*act1-122*	Cs$^-$, Ts$^-$	Recessive	Fnu4HI (+)	2	10, 11
E83A,K84A	*act1-121*	Cs$^-$, Ts$^-$	Recessive	*Bgl*II (−)	1	8
E93A,R95A	*act1-130*	Lethal	Recessive*	DNA sequence	1	10
E99A,E100A	*act1-120*	Ts$^-$	Recessive	Fnu4HI (+)	1	10
R116A,E117A,K118A	*act1-119*	Ts$^-$	Recessive	Fnu4HI (+)	3	5, 8, 8
D154A,D157A	*act1-118*	Lethal	Partial dominant	DNA sequence	2	12, 12
R177A,D179A	*act1-129*	Ts$^-$	Recessive	ClaI (−)	2	10, 18
R183A,D184A	*act1-117*	"Wild type"		Fnu4HI (+)	1	10
D187A,K191A	*act1-116*	"Wild type"		*Bgl*II (−)	1	10
E195A,R196A	*act1-115*	"Wild type"		*Pvu*II (+)	1	10
E205A,R206A,E207A	*act1-114*	Lethal?	Dominant?	*Pst*I (+)		Not recovered
R210A,D211A	*act1-113*	Weak Ts$^-$	Recessive	Fnu4HI (+)	1	10
K213A,E214A,K215A	*act1-112*	Cs$^-$, Ts$^-$[f]	Recessive	Fnu4HI (+)	3	8, 9, 10
D222A,E224A,E226A	*act1-111*	Ts$^-$	Recessive	*Bst*BI (−)	1	8
E237A,K238A	*act1-110*	Lethal	Partial dominant	Fnu4HI (+)	1	10
E241A,D244A	*act1-128*	Lethal	Partial dominant	*Pvu*II (+)	2	10, 2
E253A,R254A	*act1-109*	Lethal	Partial dominant	Fnu4HI (+)	2	10, 10
R256A,E259A	*act1-108*	Cs$^-$, Ts$^-$	Recessive*	Fnu4HI (+)	1	8
E270A,D275A	*act1-127*	Lethal	Recessive*	*Hin*fI (−)	2	10, 10
D286A,D288A	*act1-107*	Lethal	Recessive*	DNA sequence	1	10
R290A,K291A,E292A	*act1-106*	Lethal	Recessive*	Fnu4HI (+)	2	8, 10
E311A,R312A	*act1-105*	Cs$^-$, Ts$^-$[f]	Recessive	Fnu4HI (+)	2	8, 8
K315A,E316A	*act1-104*	"Wild type"		Fnu4HI (+)	1	10
K326A,K328A	*act1-126*	Lethal?	Dominant?	*Nco*I (+)		Not recovered
E334A,R335A,K336A	*act1-103*	Lethal	Recessive*	Fnu4HI (+)	2	9, 10
K359A,E361A	*act1-102*	"Wild type"		DNA sequence	4	8, 9, 9, 10
D363A,E364A	*act1-101*	Ts$^-$	Recessive*	Fnu4HI (+)	1	10

[a] In all cases the indicated mutation is linked to the downstream *HIS3* transforming marker.
[b] Cs$^-$ = cold sensitive, Ts$^-$ = heat sensitive.
[c] Method used to detect the allele; restriction enzyme used when a cut site is either created (+), or destroyed (−); DNA sequence indicates no sites are changed.
[d] The number of independent transformants dissected.
[e] Each numeral represents spores derived from separate single colony isolate.
[f] Low spore viability.

HIS3 gene, there would be several possible outcomes. In one of these the constructed *act1* mutation, despite the short distance, becomes separated from the *HIS3* marker by recombination. This case would be difficult, especially in a diploid, to distinguish from successful insertion of a recessive *act1* mutation. To avoid this problem, we marked one of the *act1* genes in the recipient diploid with a deletion-substitution that replaces most of the *ACT1* coding sequence with the *LEU2* gene (Figure 2B). All the *ACT1* coding material from the intron near the beginning of the gene to the *Bcl*I site downstream is removed. In a strain heterozygous for this allele (*act1Δ1::LEU2*), transformation with a wild-type *ACT1*-containing *Eco*RI fragment from pKFW46 that extends beyond the intron at the 5′ end and beyond the *Bcl*I site downstream could result in two common kinds of His$^+$ transformants: those that replace the intact *ACT1* allele (these will remain Leu$^+$) and those that replace *act1Δ1::LEU2* (these will become Leu$^-$, see Figure 2C). Since the donor *HIS3* gene is inserted at the end of the recipient's deletion (the *Bcl*I site), it is not possible for the *LEU2* marked chromosome to acquire the *HIS3* gene while retaining *LEU2*, nor is it possible to acquire wild-type *ACT1* sequences without involving the other, intact, *ACT1* allele. Therefore, by screening among the His$^+$ transformants for Leu$^-$ individuals, we can reasonably expect to have replaced the

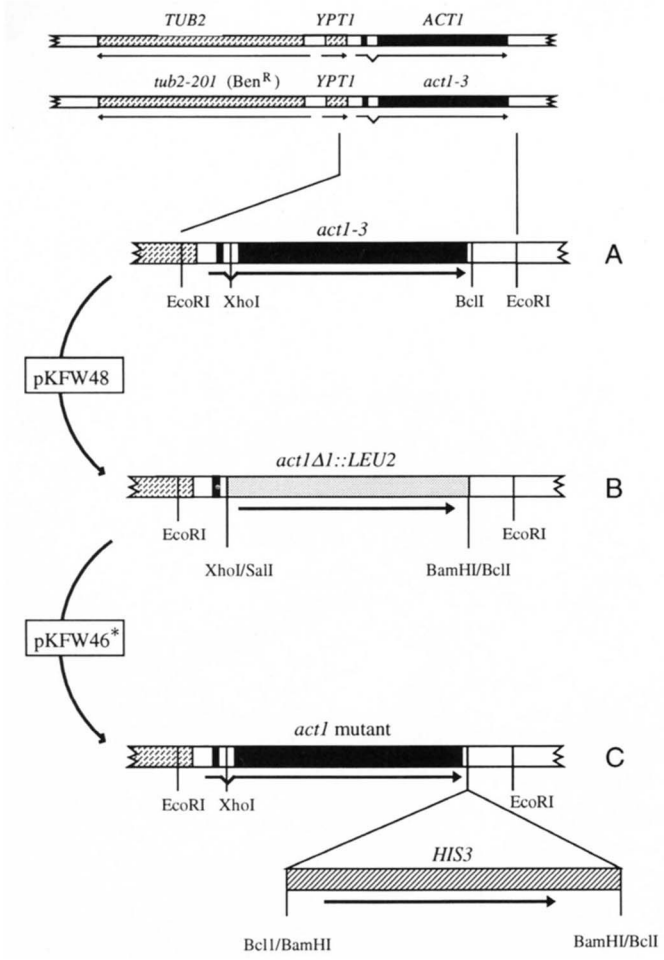

FIGURE 2.—Diagrammatic representation of constructions at the yeast *ACT1* locus. The top two lines depict the heterozygosity at the *ACT1-TUB2* locus present in the parental diploid strain KWY198 (DBY3357 × KWY175). The three enlarged lower views (A–C) illustrate events occurring upon the *act1-3* bearing homologue and represent the different genomic arrangements employed in these experiments. In preparation for gene replacement experiments, the *act1-3* allele (A) was deleted and replaced with the *LEU2* gene (B). Subsequently, the marked *act1* deletion was replaced by transformation using plasmid borne mutant copies of *act1* (C). See MATERIAL AND METHODS for a detailed description.

act1Δ1::LEU2 allele with the mutated *act1::HIS3* from the plasmid.

To provide even more genetic control over the situation, we included in the recipient another marker closely linked to *act1Δ1::LEU2*: *tub2-201*, an allele that confers recessive resistance to the antimicrotubule drug benomyl (THOMAS, NEFF and BOTSTEIN 1985). Thus, a simple substitution of our mutated *act1::HIS3* for the *act1Δ1::LEU2* should leave our mutation (and *HIS3*) linked to the *tub2-201*(Ben^R). As described below, this was generally what we observed. In some cases, however, more complicated outcomes were observed, especially when we attempted to introduce (via His$^+$ selection) an *act1* allele that turned out to be severely defective and/or partially dominant.

The diploid strain that served as a recipient of the mutant alleles (KWY201, see MATERIALS AND METHODS for construction details) had the following genotype:

$$\frac{MAT\mathbf{a}\ \ ACT1\qquad\qquad TUB2\ \ his3\Delta\ \ leu2\ \ ura3}{MAT\alpha\ act1\Delta1::LEU2\ tub2\text{-}201\ his3\Delta\ leu2\ ura3}$$

$$\frac{ade2\ \ can1\ \ cry1\ \ ADE4}{ADE2\ CAN1\ CRY1\ ade4}$$

Upon repeated tetrad dissection, this strain showed the clear recessive lethality of the *act1Δ1::LEU2* allele (0/20 Leu$^+$), and the viable spores were rarely benomyl-resistant (1/20 Ben segregants), indicating the expected low frequency of recombination bringing the *ACT1* wild-type allele together with *tub2-tub2-201*. When KWY201 was transformed with an unmutagenized linear *ACT1::HIS3* fragment from pKFW46, approximately 20% of the His$^+$ transformants had concomitantly become Leu$^-$. Individual His$^+$/Leu$^-$ transformants, when dissected (Figure 3), showed high spore viability (113/120), and 2:2 segregation for all phenotypes (including His$^+$ and Ben^R). The haploid segregants of these transformants were uniformly healthy and demonstrated no new phenotypes with regard to growth at high or low temperatures on YEPD medium (or YEPD + 900 mM NaCl, of later relevance).

Recovery and verification of mutants: To verify that the His$^+$/Leu$^-$ transformants had the mutated *act1::HIS3* construction integrated at the *ACT1* locus,

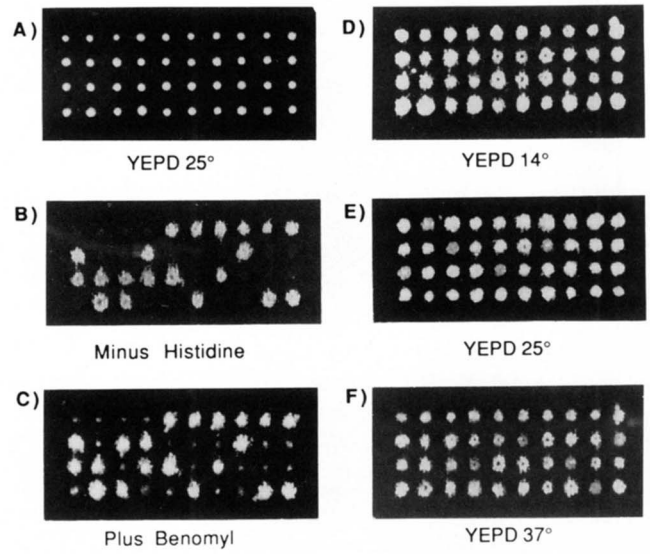

FIGURE 3.—Dissection of *ACT1/ACT1::HIS3* parental diploid. Control experiment demonstrating the viability and uniformity of haploid segregants containing the *HIS3* gene insertion downstream of the *ACT1* transcriptional unit. KWY295 (*ACT1/ACT1::HIS3*) was sporulated and dissected on YEPD medium and incubated at 25° for 3 days, at which time the colonies were replica plated to the indicated conditions (see MATERIAL AND METHODS for details). His$^+$ segregants (identified in panel B) show coinheritance of benomyl resistance (*tub2-201*, panel C) and indistinguishable growth properties on YEPD across the temperature range (panels D, E and F) used for the subsequent characterization of the mutant alleles.

we used the additional length of the *HIS3* gene as an indicator in Southern blot experiments. Over the course of these experiments we examined *Eco*RI digested genomic DNA from 46 independent His$^+$/Leu$^-$ transformants using the Southern DNA hybridization technique (SOUTHERN 1975). In all cases proper replacement of *act1Δ1::LEU2 was* indicated by the presence of both wild-type (3.8 kb) and *HIS3* insert bearing (5.8 kb) *Eco*RI restriction fragment lengths (Figure 4C, lane 1).

To verify the presence of the mutation on the chromosome, we took advantage, once again, of the inserted *HIS3* gene. As described in the MATERIALS AND METHODS, we amplified the *ACT1* sequences adjacent to *HIS3* using genomic DNA from the transformants in a PCR, using one primer upstream of the *ACT1* gene and another, antisense primer at the beginning of the *HIS3* gene (Figure 4A). In this way we amplified, from the heterozygote, only the actin sequences adjacent to the inserted *HIS3* gene, where the mutations should lie. For those mutations that involved the gain or loss of a restriction site at the mutation site (see Table 2), amplified fragments were then digested with the appropriate enzyme and the presence of the mutation was confirmed by agarose gel electrophoresis (see examples in Figure 4B).

Tetrads from these transformants (in many cases two or more isolates derived from independent bacterial plasmids; see materials and methods) were then dissected and segregants were examined. These data provided final confirmation of the high fidelity of this genomic replacement strategy: segregation analysis of 65/74 independent transformants showed in all cases (618 tetrads) strong genetic linkage between the transforming *HIS3* marker and the resident *tub2-201* allele. In the other nine cases, linkage could not be assessed because the transformants analyzed were homozygous for either the *HIS3* or *TUB2* markers. Most importantly, coinheritance of *HIS3* and the mutant *act1* allele was absolute for transformants with all except two of the thirty alleles detectable by restriction site analysis, and these two (*act1-114* and *act1-126*) showed other informative anomalies (see below). We did not attempt to demonstrate conclusively the coinheritance of the *act1* mutation with *HIS3* for those few alleles that do not create or destroy restriction sites. Nonetheless, in each case the combined evidence, with respect to allele length, segregation analysis, and phenotypic corroboration by independent mutant constructs, argued strongly that these mutations were also properly introduced. Typically, we tested the products of at least eight tetrads for each allele, in each case scoring the segregation of all known markers (except *cry1*, which is linked to *MAT***a** in KWY201). In addition, we examined the growth of these strains across a broad temperature range (11–37°) under

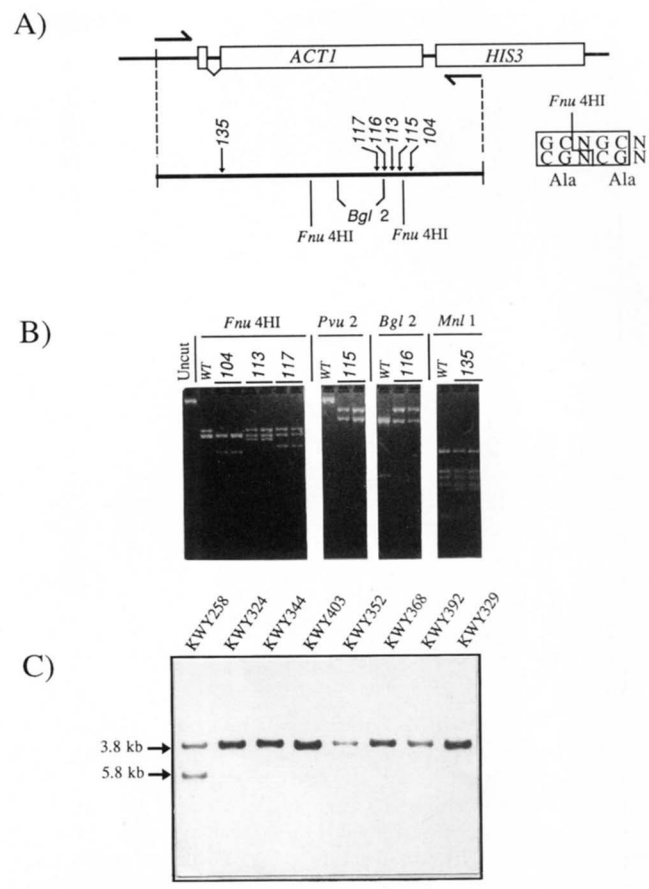

FIGURE 4.—Detection of mutations on the yeast genome. Verification of mutation on the yeast genome by PCR amplification of *HIS3*-linked actin coding sequences from heterozygous diploids. (A) Oligonucleotide primers (half arrowheads), homologous to *ACT1* upstream sense and *HIS3* upstream antisense sequences, were used to prime DNA synthesis on genomic DNA from strains bearing *HIS3*-linked act1 alleles (identified by allele number in panels A and B). The inset shows the generation of a new Fnu4HI site due to the introduction of consecutive alanine codons. (B) DNA fragments generated by PCR as above were used for diagnostic restriction enzyme digestion and analysis by agarose gel electrophoresis. Shown are six such determinations. For each mutant allele, two independent transformants are shown; for each enzyme the extreme left lane is wild-type control. As noted in the text and in Table 2, most mutations either remove of create restriction endonuclease sites and can be detected as an altered restriction pattern. (C) Southern DNA hybridization experiments, using DNA probes derived from actin coding sequences, were routinely used to confirm heterozygousity at *ACT1* (3.8-kb wild-type and 5.8-kb *act1::HIS3 Eco*RI fragments). His$^+$/Leu$^-$ diploid transformants show the expected *Eco*RI length polymorphism (*e.g.*, KWY258), while His$^+$ haploid segregants of such strains (KWY324, 344, 403, 352, 368, 392 and 329) contain only the longer, *HIS3* marked allele.

normal cultural conditions (YEPD), and with osmotic challenge (YEPD + 900 mM NaCl).

Phenotypic characterization of the mutants: We began the characterization of the new actin mutants by comparing the properties of the heterozygous diploids to the diploid heterozygous for the *act1* null mutant (their immediate parent) and a wild-type control transformant (*ACT/ACT1::HIS3*). Diploid cells

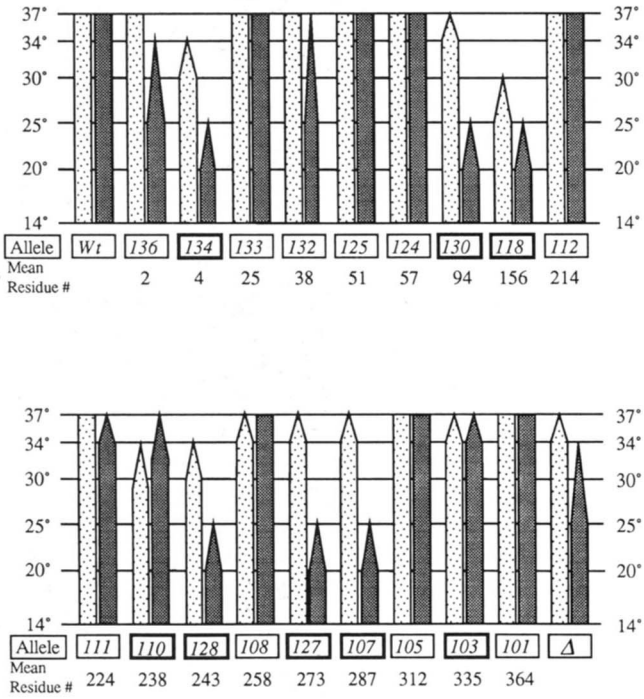

FIGURE 5.—Growth of *act1::HIS3/ACT1* heterozygous diploid strains. The range of temperatures at which mutants can grow is shown by the presence of the bars. The taper at the ends of individual bars in this chart is used to represent the degree of growth impairment with respect to temperature for heterozygous mutant strains, relative to wild-type, on YEPD (light stippled bars), or YEPD + 900 mM NaCl (solid bars) at each indicated temperature. Pointed ends on bars are used when growth at the indicated temperature is very poor, but detectable. The *act1* allele present in combination with wild type is indicated by the boxed number; **bold boxes** are used for alleles that are lethal in haploid cells. "Mean residue #" refers to the rounded average of the positions of the alanine substitutions in the actin protein sequence. Not all alleles are shown: the selection was made to illustrate the range of phenotypes seen in heterozygotes.

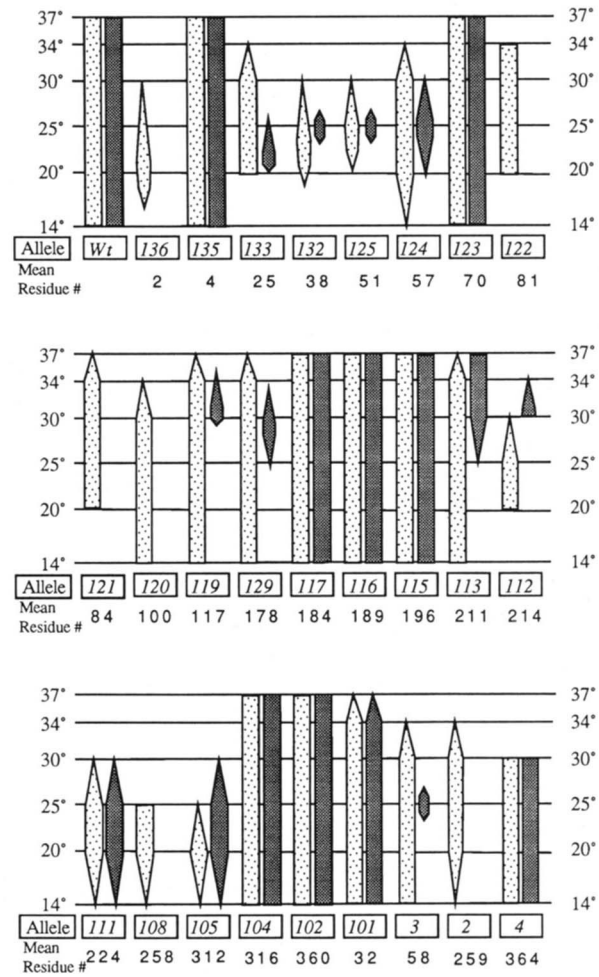

FIGURE 6.—Growth of *act1* mutant haploid strains. The range of temperatures at which mutants can grow is shown by the presence of the bars. The taper at the ends of individual bars in this chart is used to represent the degree of growth impairment with respect to temperature for *act1::HIS3* cells, relative to wild-type, on YEPD (light stippled bars), or YEPD + 900 mM NaCl (solid bars). Pointed ends on bars are used when growth at the indicated temperature is poor, but detectable. "Mean residue #" refers to the rounded average of the positions of the alanine substitutions in the actin protein sequence. All viable haploid alleles are shown.

containing only a single actin gene (*ACT1/act1Δ1::LEU2;* hereafter referred to as the hemizygote) grow poorly at 37° (Figure 5). This weak temperature sensitivity (Ts^-) is augmented by addition of 900 mM NaCl to the medium, resulting in a total inhibition at 37°, poor growth at 34°, and lesser effects detectable at temperatures as low as 30°. Control diploid cells (*ACT1/ACT1::HIS3*) show no growth inhibition regardless of incubation temperature or osmotic challenge. We used these properties of the hemizygote, a strain with half the functional actin dosage, as a benchmark for the comparison of strains heterozygous for the new *act1* mutations. Such tests implied considerable residual function for many of the mutant proteins. Partial function was evident in one of two ways, either heterozygotes grew better than the hemizygote at 37°, or they displayed greater temperature or osmotic sensitivity.

Temperature-sensitive alleles: Haploid cells containing 16 of the 36 alleles are temperature sensitive for growth (Figures 6 and 7). Nine of the Ts^- mutants are also cold sensitive (Cs^-). The permissive temperature ranges and the severity of the Ts^- phenotypes vary considerably for cells carrying different alleles. For example, some alleles (*act1-101*, *act1-124*, *act1-122*, *act1-120*, *act1-119* and *act1-129*) allow good growth well into the higher temperature range (34°). Other alleles allow very narrow permissive ranges, with best growth near 20° (*act1-108*, *act1-111*, *act1-125*, *act1-133* and *act1-136*). We found no alleles that were Cs^- and not also Ts^-.

The response of cells bearing the the Ts^- alleles to osmotic challenge was also diverse. Many failed to grow at all on YEPD containing 900 mM NaCl (Figure 6). High salt narrowed the permissive growth range for some mutants (*e.g.*, *act1-124* and *act1-129*), in some cases in an asymmetric fashion (compare *act1-119* with *act1-133*). The Ts^- phenotype of two mutants (*act1-*

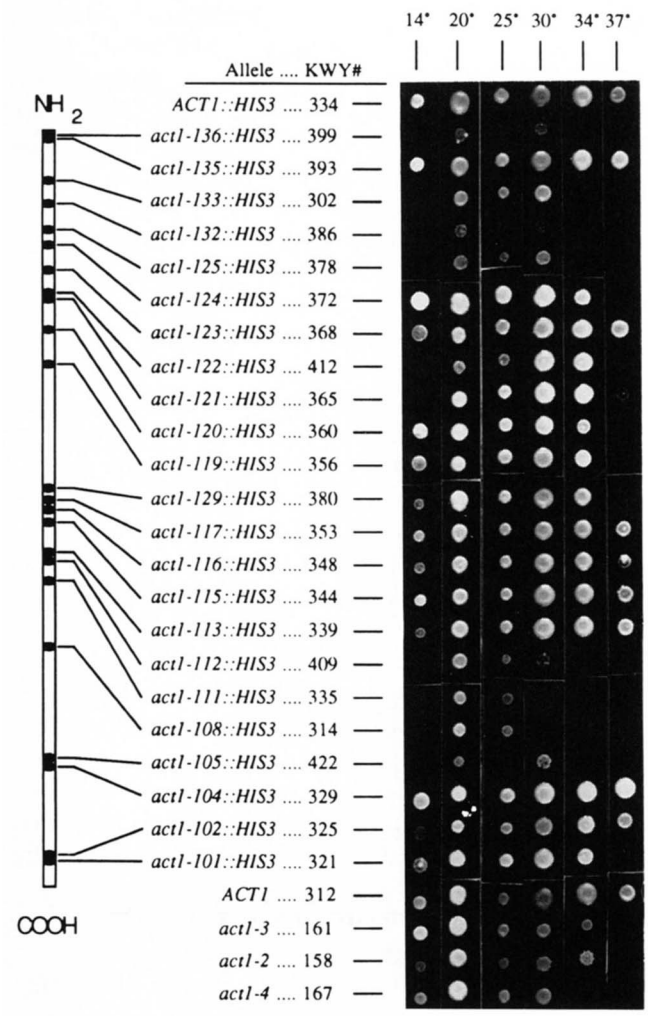

FIGURE 7.—Demonstration of the growth properties of haploid *act1* mutant strains. Uniform suspensions of cells were spotted on the surface of YEPD agar plates and incubated at the indicated temperatures. Relative health of a strain at a given temperature is judged by direct comparison of its growth to either wild-type control strain (KWY334 and KWY312). Plates incubated at different temperatures were photographed different times to yield a more uniform extent of growth for the wild-type controls.

105 and *act1-112*) was suppressed by NaCl at 30°. In contrast, salt addition had no effect upon the temperature profiles of strains bearing *act1-101* or *act1-111*.

When tested as **a**/α heterozygotes, we found that almost all all heterozygotes for Ts$^-$ alleles grew as well as homozygous wild-type **a**/α diploid cells at all temperatures (examples in Figure 5). That is, with the possible exception of *act1-108*, they were all fully recessive. In contrast, as mentioned above (see also Figure 5) diploids bearing the null *act1Δ1* and wild-type alleles show a weak growth-failure phenotype at 37°. These results, taken together, suggest that each of these Ts$^-$ mutations allows some function (*i.e.*, more than null) by the mutant allele in heterozygotes with *ACT1*. This is notable because several of these alleles (*e.g.*, *act1-105*, *act1-132* and *act1-136*), as haploids, fail to grow as well as wild-type haploids at any temperature.

Recessive lethal alleles: Almost one third (11/36) of the mutations we constructed resulted in a recessive defective phenotype causing 2:2 segregation of lethality in tight linkage with *HIS3* and *tub2-201* (Ben^R). Upon examination of the fate of the "dead" spores by light microscopy, we found that all of these cells had initiated germination, as judged by cell size and refractility in the light microscope. Some alleles showed a few to several rounds of budding prior to arrest (*e.g.*, *act1-103*, for which we found clumps of 5–200 cells), but most never budded, appearing as a single swollen cell. This latter result is similar to the null phenotype, as determined by control dissections of the *ACT1/act1Δ1::LEU2* parent.

These results, of course, speak only to the viability of these mutants under our standard dissection conditions (YEPD at 25°). In anticipation of a large lethal mutant class, we designed our transformation strain to allow rapid screening for permissive conditions. We did this by including several recessive drug resistance markers in the transformation recipient (*can1*, *cry1* and *tub2-201*) to permit the bulk selection of haploid segregants as random spores. However, we were unable to find permissive conditions for any of these mutants when plating random spore suspensions (ROCKMILL, LAMBIE and ROEDER 1991) under His$^+$ and Can^R selection (*act1-X::HIS3*, *can1* haploids).

Despite their otherwise uniform behavior, these recessive lethal alleles can be distinguished from one another by examination of the growth properties of the original heterozygous diploid transformants. About half of these alleles (Figure 5, and Table 2) behave like the null allele in the heterozygous state: they grow poorly at 37°. We have termed this behavior "recessive*" to distinguish it from the truly recessive properties of the Ts$^-$ class described above. In contrast, strains heterozygous for the remainder of the defective alleles are more temperature sensitive than the hemizygote. The degree of this "partial" dominance varies by allele (Figure 5): heterozygotes of *act1-118* and *act1-134* being the most, and *act1-128* or *act1-131* the least, dramatically affected.

Potentially dominant lethal alleles: We have been unable to recover transformants containing two of the alleles (*act1-114* and *act1-126*) we constructed. The analysis of these failed attempts uncovered several unusual results. First, when donor fragments containing either *act1-114* or *act1-126* were used for transformation, the frequency of Leu$^-$ isolates among His$^+$ transformants was 1–2%, about 10-fold reduced relative to the transformation results with all other alleles; the frequency of total His$^+$ transformants was not significantly reduced. Second, PCR amplification and restriction site analysis demonstrated that none of these relatively rare His$^+$/Leu$^-$ isolates (0/8 tested) contained what should have been the linked *act1*

allele. Finally and tellingly, tetrad analysis revealed unexpectedly that these transformants (4/4) had become homozygous at the flanking *TUB2* locus. This latter result suggests the participation of the resident, intact, *ACT1* allele in the event that replaced *act1Δ1-LEU2*. Taken together these results strongly suggest that *act1-114* and *act1-126* are dominant lethal alleles. Direct demonstration of dominant lethality will require ectopic expression experiments; such experiments, made unusually complex by the fact that overproduction of wild-type actin is often lethal, are underway.

Mutant alléles with no detectable mutant phenotype: Seven of the alleles we constructed demonstrated no detectable phenotype either as haploids or heterozygous diploids under any of the temperature or osmotic conditions we employed. For five of these alleles it was possible to detect the presence in yeast of the mutation by the combination of PCR amplification and restriction site analysis: results with several of these alleles (*act1-104*, *act1-115*, *act1-116*, *act1-117* and *act1-135*) are shown in Figure 4B. It is therefore absolutely clear that these mutations were properly recombined onto the chromosome. Upon subsequent tetrad analysis, all displayed 2:2 segregation and genetic linkage to *HIS3* and *tub2*.

We cannot be as certain about the remaining two alleles (*act1-102* and *act1-123*). In each case we analyzed four independent transformants representing two independent mutant plasmid constructs. In every case His^+ segregated 2:2, and these haploids were shown by DNA hybridization blots to contain the expected 5.8-kb actin allele.

DISCUSSION

When we began this work, only three different mutant alleles of actin had been isolated, all by some form of limited random mutagenesis *in vitro* of the *ACT1* gene and subsequent replacement of the wild-type copy in the yeast genome with the mutagenized one (SHORTLE, NOVICK and BOTSTEIN 1984; T. DUNN and D. SHORTLE, unpublished result). In numbers, these mutants were a disappointing yield of considerable effort in two laboratories. We previously argued that the low yield might be related to the strong conservation of the actin sequence in evolution; *i.e.*, due to functional constraints most mutations would be effectively lethal. Using charged-to-alanine scanning mutagenesis we recovered 34 of the 36 mutants we attempted to make, including 11 recessive lethals, 16 conditional-lethals and 7 with no discernible phenotype. These results suggest that there is no insurmountable functional constraint, since most regions of the actin gene are readily mutable using an appropriate systematic approach.

Advantages of scanning mutagenesis methods: Our new approach to the generation and evaluation of mutations in the yeast *ACT1* gene offers many advantages over more traditional mutagenesis schemes. By the nature of their construction, site specific mutations are known commodities. Strategies employing random mutagenesis (even those restricting the region of mutagenesis) rely on the often laborious phenotypic identification of mutants for final confirmation of a successful mutagenesis. This is not a trivial point, especially when relying on a mutant allele to provide an essential function. In this circumstance, a failure to identify mutants has many interpretations, including technical concerns about the mutagenesis reaction, the conditions used for recovery of transformants and the tests employed for the detection of mutant phenotypes. Despite its advantages, site-specific mutagenesis as usually employed is an inherently biased method requiring explicit selection of target sites; mutations not targeted in advance are never obtained. To achieve a survey of mutation possibilities, while still enjoying the advantages of a site-directed approach, we "scanned" the actin gene, targeting sites on the basis of their chemical properties alone.

In our scanning approach we employed two rules, both directed at minimizing the number of alleles that grossly alter the folded structure of the molecule. The first was to change charged residues in regions where they are clustered. The idea behind this is to bias the collection toward alteration of the surface of the molecule, effectively reducing the number of alleles that do violence to the hydrophobic core of the protein. As discussed below, this idea has been validated in our case by the subsequently published actin:DNase I cocrystal structure (KABSCH *et al.* 1990). The second principle we employed was to make all replacements with the small, uncharged amino acid, alanine. Changes of charged residues to alanine, in effect, simply truncate an amino acid's side chain at its β-carbon. We think it likely that both of these considerations played major roles in our successful recovery of 23 new haplo-sufficient alleles.

An alternative to a structure-based scanning approach would be to target mutations to putative functional sites implicated by biological experimentation. JOHANNES and GALLWITZ (1991) have recently reported the results of just such a study with the yeast *ACT1* gene. Their collection of alleles altered residues identified as possible binding sites for a variety of factors, including actin, myosin and ATP. Surprisingly, 11 of the 13 replacement alleles that they constructed show no phenotype even in haploid cells. The remaining two are apparently dominant lethal substitutions. It would seem that in the case of even an extensively characterized protein like actin, the existing literature offered little guidance toward the gen-

eration of genetically useful mutations. Thus, although site-directed mutagenesis based on prior experimentation offers tremendous corroborative potential, at the same time, it provides very limited opportunity for new and possibly unpredictable discoveries. A scanning strategy, in contrast, can serve both to corroborate and to discover, because of its synoptic nature. Finally, it is worth noting that scanning methods are essentially independent of the biology of the protein of interest and can be applied to any cloned gene.

Recovery of mutations in yeast and evaluation of mutant phenotypes: There were, in our experiments, many advantages to evaluating the new mutant alleles by replacement into the yeast genome that amply justified any additional labor over plasmid methods. First, it made possible the recovery and direct identification of recessive lethal alleles, distinguishing them from dominant lethal alleles. Considerable doubt would have remained about the phenotype of all defective alleles had the only criterion been failure to recover a plasmid. Second, the heterozygous initial transformants were themselves useful in presaging dominance/recessiveness relationships. The heterozygotes also allowed us to detect residual function of recessive lethal alleles. Perhaps most importantly, our chromosome-based strategy eliminated concerns about gene dosage effects that inevitably accompany any plasmid based strategy. Having the mutations in single copy in their normal genetic environment seems to us nearly a necessity for dosage-sensitive genes such as *ACT1*.

Much of the control we enjoyed over the construction and interpretation of the mutations can be traced to the positioning of markers in the transforming DNA and the recipient genome. This includes both the placement of the transforming marker *(HIS3)* coincident with the downstream end point of the *LEU2* marked deletion (the 3′ flanking *Bcl*I site), and the provision of a marker at the target locus such that recombination places the mutant allele between two scorable markers (in our case; *tub2-201 act1-X::HIS3*). Because our genomic replacement and dissection strategy yielded mutations that behaved as Mendelian elements (segregating 2:2 at meiosis), we could confirm the expected cosegregation of any new phenotype with the transforming marker, and provide proof of proper integration by linkage of these traits to the resident drug-resistant *tub2* allele.

Eventually one wishes to have any new allele residing within its normal chromosomal context. With plasmid-based strategies this requires further strain construction. In contrast, the mutant haploid segregants from the analytical dissections are the final product. By using a genomic strategy, we generated as a by-product, a collection of nutritionally marked isogens of both mating types. We are now ready for further genetic analysis, including identification of interallelic complementation, synthetic lethal interactions, or suppression.

The actin crystal structure confirms most mutations are on the surface: In the course of these studies a structure for the actin:DNase I co-crystal was published (KABSCH *et al.* 1990). We can now estimate the efficiency with which the charged cluster bias actually targeted surface residues. By examination of the structure (Figure 8) one can describe the changed residues as belonging to one of three structural classes: (1) surface exposed; (2) surface, but interacting with nucleotide or divalent metal ion; or (3) buried in structure. We found that 81% (61 of 75) of the residues we changed are indeed on the surface of the crystal structure, 72% (54 of 75) being largely solvent exposed. The remaining seven residues (D11 in *act1-134*; K62 in *act1-131*; D154 and D157 both in *act1-118*; E207 in *act1-114*; E214 in *act1-112*; and E334 in *act1-103*) are involved in other ionic surface interactions (see below). All but one of these seven "interaction" residues are components of lethal substitutions, including the most extreme recessive lethal alleles, *act1-118* (D154A,D157A) and *act1-134* (D11A). Lastly, only 19% (14 of 75) of the substitutions are significantly buried in the folded structure, the yield of mutants from these being evenly distributed between Ts^- and Lethal phenotypic classes. Most of these "buried" residues are relatively superficial: only two or three might leave a destabilizing void (ERIKSSON *et al.* 1992) in the protein core upon replacement with alanine. Thus, the structural data strongly support the initial assumption that a charge bias should generate a collection enriched for surface changes and depleted of mutations that effect monomer folding (CUNNINGHAM and WELLS 1989; BENNETT *et al.* 1991; BASS, MULKERRIN and WELLS 1991; GIBBS and ZOLLER 1991).

Mutant phenotypes seen in the light of the actin structure: The structural data are helpful in interpreting the mutant phenotypes and directing future experimentation. The majority of the new Ts^- *act1* alleles (12/16) change only surface residues and are therefore unlikely to encode structurally thermosensitive proteins. We anticipate that many of these Ts^- alleles act by compromising interactions of actin with one or more of its many binding partners. For example, *act1-132* (R37A,R39A; see Figure 8), which lies near the proposed longitudinal contacts along the two-start helix of filamentous actin (HOLMES *et al.* 1990); possibly this mutation affects binding of actin to itself in the filament.

It is significant that all the temperature-sensitive alleles (except *act1-108*) behave as true recessive mutations. First, it demonstrates that these proteins are

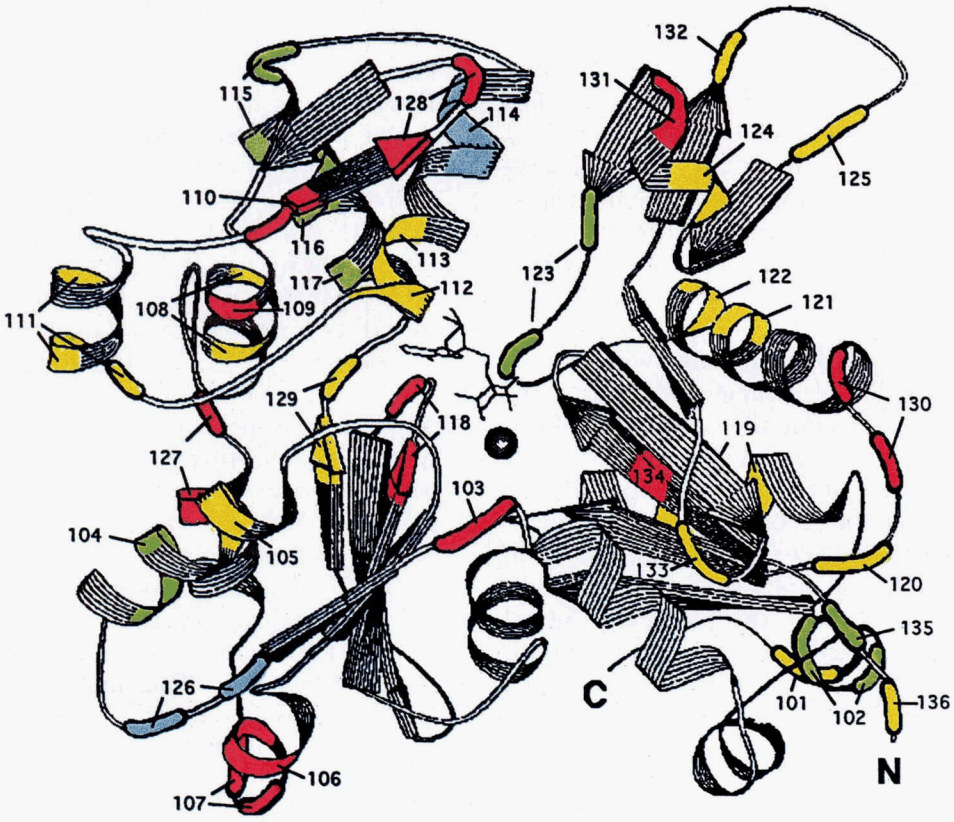

FIGURE 8.—Ribbon diagram of the actin monomer. Portions of the diagram illustrating the positions of the backbone residues for the charged-cluster replacements are color coded by haploid mutant phenotype: alleles with no phenotype, green; temperature sensitive, yellow; lethal, red; putative dominant lethal, blue. Numbers refer to allele designations. The adenine nucleotide is shown in the prominent cleft as a simple stick model and the divalent metal ion as a large filled circle. Adapted from KABSCH *et al.* (1990).

made, and can make functional contributions at the restrictive temperature. Second, it suggests that actin filaments composed of only mutant monomers lack some function(s) that are only essential at higher temperatures, and can be provided by the wild-type protein when coassembled. This makes the strong prediction that the new Ts^- alleles will be valuable tools for probing structural and functional relationships of actin binding proteins using genetic techniques. Furthermore, because alanine surface substitutions are expected to result in only localized structural changes (CUNNINGHAM and WELLS 1989), we should be able to define functional domains with considerable resolution. For example, alleles that act by reducing (or increasing) the filament surface affinity for a particular binding protein should be suppressible by a variety of means, including the alteration or overproduction of the binding partner.

The structural data offer reasonable explanations for the phenotype of the majority of the lethal alleles (see Figure 8). Four of the eleven lethal substitutions change residues shown to interact with the structurally essential divalent metal ion (*act1-134*; D11A), the bound nucleotide (*1-103* [E334A,R335A,K336A] and *act1-112* [K213A,E214A,K215A]), or both (*act1-118* [D154A,D157A]). Two of the alleles alter residues that interact with one another, apparently forming a salt bridge across the top of the nucleotide binding cleft (K62A in *act1-131* and and E207A in *act1-114*).

A few of the defective alleles may affect actin filament assembly since, like *act1-132* mentioned above, they reside in areas modeled as contact sites along the two-start helical filament path (HOLMES *et al.* 1990). These include the recessive alleles *act1-106* (R290A,K291A,E292A), *act1-107* (D286A,D288A), *act1-128* (E241A,D243A), and the two inferred dominant lethal alleles *act1-114* (E205A,R206A,E207A) and *act1-126* (K326A,K328A). The dominance of the latter alleles (colored blue in Figure 8) may be explained mechanistically by the ability of the mutant monomers to add to growing filaments, while blocking subsequent monomer addition. In the parlance of actin biochemistry these would be capping proteins: *act1-114* and *1-126* capping the pointed and barbed ends of the filament, respectively.

Only two of the remaining recessive lethal mutations (*act1-109* [E253A,R254A] and *act1-127* [E270A,D275A]) change residues that are buried in structure (Figure 8), and therefore might influence proper folding. The strong correlation of lethal phenotype with sites of known functional importance points to the likely significance of the remaining two

lethal substitutions, both of which truncate side chains that are on the surface of the filament. Specifically, *act1-130* [E93A,E95A] is situated under the "footprint" that myosin makes on actin filaments (HOLMES *et al.* 1990; MILLIGAN, WHITTAKER and SAFER 1990), and *act1-110* (E237A,K238A) changes two solvent exposed groups in a region where tropomyosin is believed to bind (MILLIGAN, WHITTAKER and SAFER 1990).

Aside from their role in defining functionally important sites, the lethal alleles are valuable starting material for the identification of new conditional mutations. Conditional alleles might be found by making the corresponding single alanine replacements. However, a more powerful alternative would be to use the residues identified by the lethal substitutions as targets for random replacement (PALZKILL and BOTSTEIN 1992). Libraries of transformants containing random substitutions at these sites could be screened for new conditional phenotypes. This should provide strains altered in the suspect activity. For example, the recovery of conditional revertants for *act1-103*, *act1-112* or *act1-118* should yield proteins with aberrant nucleotide hydrolysis or exchange properties, while similar studies of *act1-106*, *act1-107* or *act1-128*, would be expected to provide alleles encoding assembly defective proteins.

As with the other phenotypic classes, some generalities can be made about the structural context of the replacements that yield no discernible phenotype. As might be expected, these mutations all change surface residues (Figure 8). Interestingly, four of these six alleles (*act1-115* [E195A,R196A], *act1-116* [D187A,K191A], *act1-117* [R183A,D184A], and *act1-123* [R68A,E72A]) change residues that lie on the face of the protein closest to the filament axis, and thus, they would be unavailable for filament surface interactions according to the model of HOLMES *et al.* (1990). Since these altered actins function normally, it suggests that these residues do not contribute significantly to filament assembly or stability. This conclusion is consistent with both the filament model, and with electron density data on negatively stained actin filaments (BREMER *et al.* 1991; and references within). The other two alleles (*act1-102* [K359A,E361A] and *act1-104* [K315A,E316A]) are expected to be on the filament surface. One of these two alleles (*act1-135* [D2A]) lies within one of the few regions where actin sequences are known to display modest divergence (HIGHTOWER and MEAGHER 1986).

In conclusion, charged-to-alanine scanning mutagenesis followed by recovery of mutations on the yeast genome has allowed us to assemble an unbiased synoptic set of mutations covering much of the surface of the actin monomer. The assumptions underlying the method have been supported both by the high yield of recovered mutations (94%) and by examination, in the three-dimensional structure of the protein, of the residues affected, 81% of which are at or near the surface. The phenotypic diversity within this collection indicates that many of the mutants should be immediately useful to geneticists and biochemists whereas others can now be made useful by further mutagenesis.

We wish to thank our colleagues A. ADAMS, G. BARNES, C. CHAN, D. EISENBERG, K. HENNESSY, M. MARINUS, D. MOUNT, P. NG, T. PALZKILL, D. PREUSS, J. WELLS, M. ZOLLER and many others who generously provided strains, ideas and advice. Our extreme gratitude is extended to W. KABSCH, H. MANNHERZ, D. SUCK, E. PAI and K. HOLMES for providing (in a most timely fashion) the coordinates of the actin:DNase I co-crystal and actin filament models. We are especially grateful to J. KIRSCH and D. KOSHLAND for providing valuable computing resources that were used for protein structure analysis. This work was supported in part by grants to D.G.D. from the National Institute of General Medical Sciences (GM42759) and the Searle Scholars Program/The Chicago Community Trust.

LITERATURE CITED

ADAMS, A. E., and D. BOTSTEIN, 1989 Dominant suppressors of yeast actin mutations that are reciprocally suppressed. Genetics **121:** 675–83.

ADAMS, A. E., D. BOTSTEIN and D. G. DRUBIN, 1991 Requirement of yeast fimbrin for actin organization and morphogenesis *in vivo*. Nature **354:** 404–408.

BASS, S. H., M. G. MULKERRIN and J. A. WELLS, 1991 A systematic mutational analysis of hormone-binding determinants in the human growth hormone receptor. Proc. Natl. Acad. Sci. USA **88:** 4498–502.

BENNETT, W. F., N. F. PAONI, B. A. KEYT, D. BOTSTEIN, A. J. JONES, L. PRESTA, F. M. WURM and M. J. ZOLLER, 1991 High resolution analysis of functional determinants on human tissue-type plasminogen activator. J. Biol. Chem. **266:** 5191–201.

BREMER, A., R. C. MILLONIG, R. SUTTERLIN, A. ENGEL, T. D. POLLARD and U. AEBI, 1991 The structural basis for the intrinsic disorder of the actin filament: the "lateral slipping" model. J. Cell Biol. **115:** 689–703.

CLEVES, A. E., P. J. NOVICK and V. A. BANKAITIS, 1989 Mutations in the SAC1 gene suppress defects in yeast Golgi and yeast actin function. J. Cell Biol. **109:** 2939–2950.

CUNNINGHAM, B. C., and J. A. WELLS, 1989 High-resolution epitope mapping of hGH-receptor interactions by alanine-scanning mutagenesis. Science **244:** 1081–1085.

ERIKSSON, A. E., W. A. BAASE, X.-J. ZHANG, D. W. HEINZ, M. BLABER, E. P. BALDWIN and B. W. MATTHEWS, 1992 Response of a protein structure to cavity-creating mutations and its relation to the hydrophobic effect. Science **255:** 178–183.

GALLWITZ, D., F. PERRIN and R. SEIDEL, 1981 The actin gene in the yeast *Saccharomyces cerevisiae*: 5′ and 3′ end mapping, flanking, and putative regulatory sequences. Nucleic Acids Res. **9:** 6339–6350.

GALLWITZ, D., and I. SUERS, 1980 Structure of a split yeast gene: complete nucleotide sequence of the actin gene in *Saccharomyces cerevisiae* Proc. Natl. Acad. Sci. USA **77:** 2546–2550.

GIBBS, C. S., and M. J. ZOLLER, 1991 Rational scanning mutagenesis of a protein kinase identifies functional regions involved in catalysis and substrate interactions. J. Biol. Chem. **266:** 8923–31.

GREER, C., and R. SCHECKMAN, 1982 Actin from *Saccharomyces cerevisiae*. Mol. Cell. Biol. **2:** 1270–1278.

HIGHTOWER, R. C., and R. B. MEAGHER, 1986 The molecular evolution of actin. Genetics **114:** 315–332.

HOFFMAN, C. S., and F. WINSTON, 1987 A ten-minute DNA preparation from yeast efficiently releases autonomous plasmids for transformation of *Escherichia coli*. Gene **57:** 267–72.

HOLM, C., T. GOTO, J. C. WANG and D. BOTSTEIN, 1985 DNA topoisomerase II is required at the time of mitosis in yeast. Cell **41:** 553–563.

HOLMES, K. C., D. POPP, W. GEBHARD and W. KABSCH, 1990 Atomic model of the actin filament. Nature **347:** 44–9.

HUFFAKER, T. C., J. H. THOMAS and D. BOTSTEIN, 1988 Diverse effects of β-tubulin mutations on microtubule formation and function. J. Cell Biol. **106:** 1997–2010.

ITO, H., Y. FUKUDA, K. MURATA and A. KIMURA, 1983 Transformation of intact yeast cells treated with alkali cations J. Bacteriol. **153:** 163–168.

JOHANNES, F. J., and D. GALLWITZ, 1991 Site-directed mutagenesis of the yeast actin gene: a test for actin function *in vivo*. EMBO J. **10:** 3951–3958.

KABSCH, W., H. G. MANNHERZ, D. SUCK, E. F. PAI and K. C. HOLMES, 1990 Atomic structure of the actin:DNase I complex. Nature **347:** 37–44.

KASSIR, Y., and G. SIMCHEN, 1991 Monitoring meiosis and sporulation in *Saccharomyces cerevisiae*. Methods Enzymol. **194:** 94–110.

KRON, S. J., D. G. DRUBIN, D. BOTSTEIN and J. SPUDICH, 1992 Yeast actin filaments display ATP-dependent sliding over surfaces coated with rabbit muscle myosin. Proc. Natl. Acad. Sci. USA **89:** 4466–4470.

KUNKEL, T. A., J. D. ROBERTS and R. A. ZAKOUR, 1987 Rapid and efficient site-specific mutagenesis without phenotypic selection. Methods Enzymol. **154:** 367–82.

MA, H., S. KUNES, P. J. SCHATZ and D. BOTSTEIN, 1987 Plasmid construction by homologous recombination in yeast. Gene **58:** 201–16.

MANIATIS, T., E. F. FRITSCH and J. SAMBROOK, 1982 *Molecular Coloning: A Laboratory Manual*. Cold Spring Harbor Laboratory, Cold Spring Harbor, N.Y.

MILLIGAN, R. A., M. WHITTAKER and D. SAFER, 1990 Molecular structure of F-actin and location of surface binding sites. Nature **348:** 217–21.

NG, R., and J. ABELSON, 1980 Isolation of the gene for actin in *Saccharomyces cerevisiae*. Proc. Natl. Acad. Sci. USA **77:** 3912–3916.

NOVICK, P., and D. BOTSTEIN, 1985 Phenotypic analysis of temperature-sensitive yeast actin mutants. Cell **40:** 405–416.

NOVICK, P., B. C. OSMOND and D. BOTSTEIN, 1989 Suppressors of yeast actin mutations. Genetics **121:** 659–74.

PALZKILL, T., and D. BOTSTEIN, 1992 Probing β-lactamase structure and function using random replacement mutagenesis. Proteins Struct. Funct. Genet. (in press).

POLLARD, T. D., and J. A. COOPER, 1986 Actin and Actin Binding Proteins. A critical evaluation of mechanisms and functions. Annu. Rev. Biochem. **55:** 987–1035.

ROCKMILL, B., E. J. LAMBIE and G. S. ROEDER 1991 Spore enrichment. Methods Enzymol. **194:** 146–148.

ROSE, M. D., F. WINSTON and P. HEITER 1990 *Methods in Yeast Genetics: A Laboratory Course Manual*. Cold Spring Harbor Laboratory, Cold Spring Harbor, N.Y.

SAIKI, R. K., D. H. GELFAND, S. STOFFEL, S. J. SCHARF, R. HIGUCHI, G. T. HORN, K. B. MULLIS and H. A. ERLICH, 1988 Primer-directed enzymatic amplification of DNA with a thermostable DNA polymerase. Science **239:** 487–91.

SANGER, F., S. NICKLEN and A. R. COULSON, 1977 DNA sequencing with chain-terminating inhibitor. Proc. Natl. Acad. Sci. USA **74:** 5463–5467.

SHERMAN, F., and J. HICKS, 1991 Micromanipulation and dissection of asci. Methods Enzymol. **194:** 21–37.

SHORTLE, D., J. E. HABER and D. BOTSTEIN, 1982 Lethal disruption of the yeast actin gene by integrative DNA transformation. Science **217:** 371–373.

SHORTLE, D., P. NOVICK and D. BOTSTEIN, 1984 Construction and genetic characterization of temperature-sensitive mutant alleles of the yeast actin gene Proc. Natl. Acad. Sci. USA **81:** 4889–4893.

SOUTHERN, E., 1975 Detection of specific sequences among DNA fragments separated by gel electrophoresis. J. Mol. Biol. **98:** 503–517.

THOMAS, J. H., N. F. NEFF and D. BOTSTEIN, 1985 Isolation and characterization of mutations in the β-tubulin gene of *Saccharomyces cerevisiae*. Genetics **112:** 715–734.

VIEIRA, J., and J. MESSING, 1987 Production of single-stranded plasmid DNA. Methods Enzymol. **153:** 3–11.

VIEIRA, J., and J. MESSING, 1991 New pUC-derived cloning vectors with different selectable markers and DNA replication origins. Gene **100:** 189–94.

Communicating editor: E. W. JONES